Effect of the Diurnal Variation of the Convective Boundary Layer Height over Metro Manila on Pollutant Concentration

Genelita B. Tubal[1]*, Mariano Estoque[2], John Holdsworth[3], and Jose Villarin, SJ[3]
[1]Environmental Science Program, College of Science
University of the Philippines, Diliman, 1101 Quezon City, Philippines;
[2]Department of Meteorology and Oceanography
University of the Philippines, Diliman, 1101 Quezon City, Philippines;
[3]Ateneo de Manila University (ADMU), Loyola Heights, Quezon City

ABSTRACT

Air pollutants are dispersed throughout a very thin layer of the atmosphere called the boundary layer (BL), and concentrations would be influenced by the thickness of the BL. A monostatic, biaxial, vertically-pointing Mie Scattering 532 nm Nd:YAG lidar was used to observe the development of the daytime BL over Metro Manila in May 1999. The data profiles were background-subtracted, energy-normalized, and range-corrected; 20,000 profiles (30-32 minute period files) were arranged in arrays in time sequential order. A MatLab program with color enhancement capability was developed to display the range-time indicator (RTI) image to visualize the BL.

The convective BL height developed with a general pattern; it increased gradually in the early morning, rapidly from mid-morning until noontime, then slowly reaching its maximum height in the early afternoon. (The maximum height reached by the BL from 1– 4 May 1999 was 1635 m). BL height is maintained or lowered very slowly from mid-afternoon until sunset.

The BL grew higher when the surface temperature and solar radiation received was greater. Fair-weather active clouds inhibited the growth of the BL. When the relative humidity was higher, the base of the fair-weather cloud field was lower; therefore, the mean BL height was also lower. Prolonged sea breeze modified the convective BL by creating a much lower BL than when there was no sea breeze.

Around 75% of the total suspended particulates (TSP) in Metro Manila comes from traffic emissions. Traffic volume over most part of Metro Manila including the main thoroughfares near the lidar site, peaks at around 09:00 Local Standard Time (LST) and between 17:00 – 18:00 LST, although traffic volume is lower than at 09:00 LST. The traffic volume reduces to 80% from its morning peak at around noontime. The morning peak of the pollution concentration occurred earlier than that of the traffic. This could be due to the fact that the BL before 09:00 LST was much lower than after it. The pollution concentration on May 1 and 2 was reduced to less than 50% from its morning peak, a reduction much less than expected based on the traffic volume. This could be ascribed to the much higher BL around noontime. The May 2 pollution profile did not have a peak corresponding to the afternoon traffic volume peak because at that time the mean BL height was still very high. The May 3 and 4 pollution profiles were different from the two previous days, with values much greater around noontime. Pollution during those times was concentrated in a much lower layer due to the sea breeze effect.

Key words: lidar, boundary layer, sea breeze, air pollution

INTRODUCTION

Air pollutants are dispersed and transported throughout a very thin layer of the atmosphere called the boundary layer (BL), a generally turbulent region whose characteristics are directly influenced by the ground (Stull, 1988). Turbulence in the BL is primarily convectively driven during calm sunny days and mechanically driven at night or even during windy overcast days (Panofsky, 1985; Benkley & Schulman, 1979). The boundary layer driven by convection, hence called a convective boundary layer (CBL), grows from sunrise and stays until around sunset. The nocturnal or stable boundary layer (SBL) grows from around sunset through the night until around 08:00 LST (Local Standard Time) the next day when it is eroded by the young CBL. See Fig. 1.

Pollutants emitted at the surface are carried aloft by convective thermals due to turbulence in the CBL (Ferrare et al., 1991). Above the CBL is an inversion or stable layer that prevents the further movement of thermals upward. Momentum causes a thermal to overshoot the inversion base, reaching the warmer region called the free atmosphere (FA). The negatively buoyant thermal decelerates and eventually sinks back down into the CBL, which is mostly intact, trapping any pollutant and moisture within it (Stull, 1988). Thus, the stable layer acts as a barrier to the transfer of pollutants from the CBL to the FA (Beyrich & Gryning, 1998). FA air is therefore much cleaner than the aerosol laden CBL.

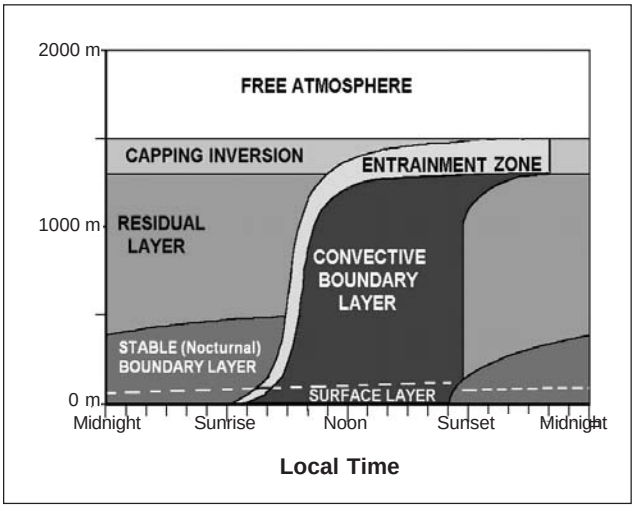

Fig. 1. The boundary layer in high-pressure regions over land consists of three major parts: a very turbulent convective boundary layer, a less turbulent residual layer, and a stable (nocturnal) boundary layer (Stull, 1988).

During the overshoot into the inversion, parcels of warm, usually drier FA air are entrained into the CBL, contributing to the increase of the CBL thickness. This region is called the entrainment zone (EZ), (Fig. 2).

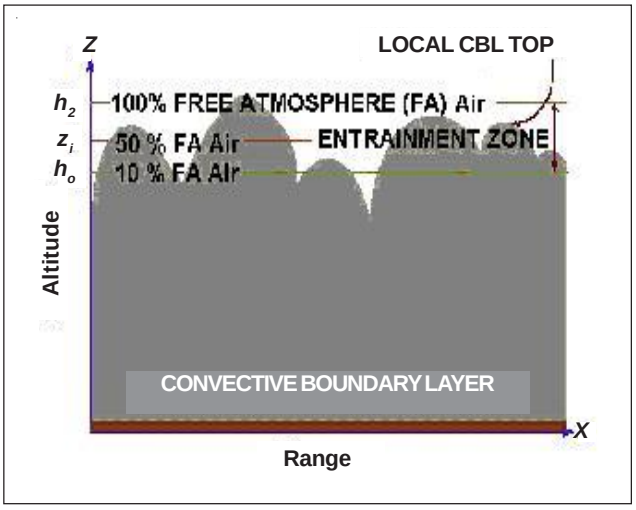

Fig. 2. The entrainment zone and the mean CBL height z_i (Stull, 1988).

A lidar, working in the same principle as radar, detects the suspended air particulates and determines clearly the extent of the CBL from a distinct drop in the return lidar signal strength at the interface between the CBL and the FA.

Sometimes convective or fair-weather clouds, can be found at the top portion of thermals. The bases of the clouds of neighboring thermals are usually at different levels because of the variability of moisture contents between thermals. The top of the CBL in a field of cloud-topped thermals is a little higher than the lowest cloud base.

During prolonged sea breeze, pollutants are trapped within a much thinner BL. This is caused by the modification of the CBL by the much lower marine

BL advected from offshore to onshore by changes in the roughness or temperature over land.

Metro Manila is under an air shed where pollutant concentrations are regularly over the standard values set by the World Health Organization (WHO) and the Philippine guidelines. Ill effects of air pollutants on human health make the study of air pollutant transport and dispersion indispensable. One of the basic parameters that need to be observed is the diurnal variation of the BL height. No observation of the BL over Metro Manila (or over any part of the Philippines) has been recorded previously.

This paper presents the results of the CBL observation on 1 - 4 May 1999 over Metro Manila using a lidar and meteorological instruments.

METHODOLOGY

Data acquisition

The Mie Scattering lidar system used in this study was situated on top (15 m agl) of the Climate Studies Building of the Manila Observatory (MO), Ateneo de Manila University, Quezon City. The MO lidar system was, at that time, monostatic, vertically pointing with biaxial configuration (Fig. 3). The axes of the laser beam and the receiver, a 28 cm-diameter Schmidt Cassegraine Telescope, were separated by 30 cm. The laser source was an Nd-YAG laser that provided 532 nm light pulses at a repetition rate of 20 Hz. The laser pulses were sent vertically to the atmosphere via dielectric mirrors after being expanded three times and collimated. The backscattered signal was received by the telescope and directed to a photomultiplier tube (PMT) via a 3-mm diameter iris, a collimating lens, a 10% transmitting neutral density filter, and 532 nm bandpass filter all positioned along the telescope optic axis.

The electrical output of the PMT was amplified 15 times by a high bandwidth operational amplifier before it was fed into a CompuScope CS1012 oscilloscope PC card. This card digitized the signal waveforms every laser pulse at a sampling rate of 20 MHz (single channel). This means that data points in one lidar data profile are 7.5 m apart. The data received was averaged to 1-second ensemble. The energy per pulse was measured by an Analog Module laser energy monitor and recorded to a PC through the DT300 data acquisition board. A LabVIEW control and data-handling program allowed the automated data acquisition from around 04:30 LST to 19:00 LST daily. A real time display of every averaged lidar profile saved unto the computer's hard disk was displayed on the monitor. With this, the alignment of the lidar system was closely monitored.

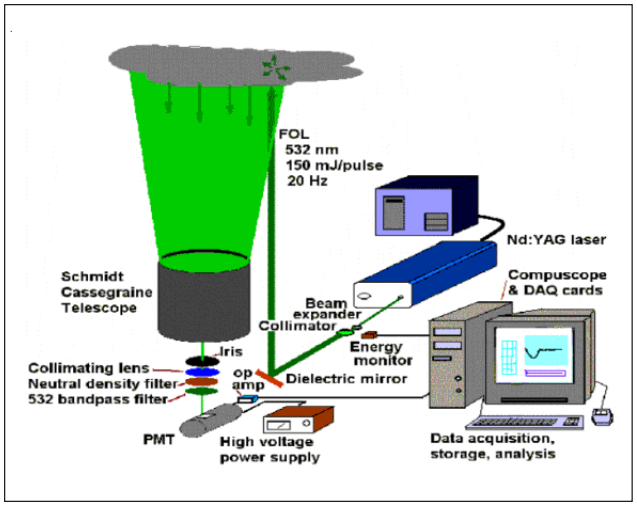

Fig. 3. Schematic diagram of the Manila Observatory lidar system.

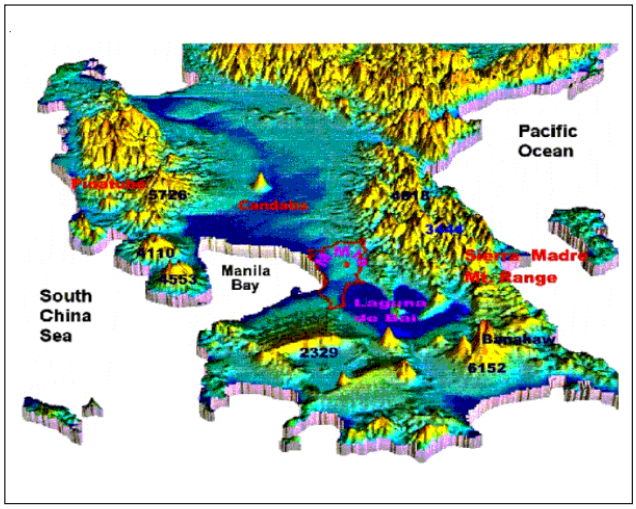

Fig. 4. Lidar site is represented by the big dot inside Metro Manila. (Map courtesy of Dr. E. Ramos of the Philippine Institute of Volcanology and Seismology (Phivolcs).)

The lidar site is situated near large bodies of water (Fig. 4). Around 14 km on its western side is Manila Bay, and around 14 km on its southeastern side is the Laguna de Bay. Metro Manila is characterized by nearly flat terrain. To characterize the meteorology of the area, surface meteorological measurements were obtained from four meteorological stations. Three were situated near the lidar site – (a) the Environmental Management Bureau (EMB) air quality monitoring van, located 50 m NE of the lidar site, which measured solar radiation, surface temperature, relative humidity, and wind speed; (b) the University of the Philippines – National Center for Transport Studies (UP NCTS) Horiba air quality monitoring van, 50 m NW of the MO lidar, which measured surface wind velocity; (c) the Philippine Atmospheric, Geophysical, and Astronomical Services Administration (PAGASA) monitoring van, situated 600 m NW of the lidar site, which measured surface temperature and wind velocity. The fourth one, (d) the PAGASA monitoring site at the Science Garden, situated 4 km NE of the lidar site, recorded wind velocity and cloud cover. Theodolite balloons were released every 1.5 hours from 6:00 LST until 18:00 LST 600 m NW of the lidar site to determine the vertical wind velocity profile. At this same site, two to three radiosondes were launched daily to determine the vertical profiles of temperature and humidity. Cloud cover was recorded every 15 minutes at the lidar site. The surface temperature used in the analysis of the CBL growth was the average of the temperature measurements obtained by the EMB and PAGASA monitoring vans. There were very slight variations between the two readings. The wind speed was the average of the wind speeds from the EMB and UP-NCTS vans. Although the two monitoring vans were very near each other, their wind speed measurements had slight variations.

Lidar data processing and analysis

The lidar data processing, done after the intensive lidar observation period, took several steps. Ten successive files of 100 profiles each were concatenated to have 1000 profiles in a bigger file with filename bearing the date and the n^{th} set of 1000 profiles. A MatLab program was developed to automatically correct each lidar profile and arrange them in an array. The correction done were subtraction of background signal, energy normalization to correct variation of laser output between laser shots, and range correction for the $1/R^2$ fall-off of laser energy. The background signal was taken to be the average value of the last 40 data points. At the range from where the data was taken (above 4.5 km), particulate matter was considered absent.

Two 1000-profile arrays were further joined to have a bigger array of 2000 profiles. This corresponds to a sampling time of about 32 minutes. Taking the average wind speed during the observation period of about 3 ms^{-1}, assuming that the convective thermals were advected across the laser beam path with this speed, then a sampling time of 32 min corresponds to sampling the CBL along a horizontal distance of about 5.7 km, a long enough range to obtain a good average of the CBL height.

A MatLab program was used to display the time sequence of the 30-minute data (2000 data profiles) in an image display called the Range-Time Indicator (RTI) map/image (Piironen & Eloranta, 1995) as shown in Fig. 5. The range of intensity was chosen such that the corresponding color scale could display the contrast of the CBL, FA, and the clouds. In Fig. 5, the dark region from 375 m and below corresponds to the height below the full overlap (FOL) of the lidar where it could not detect any scatterers. The lighter regions above the FOL region correspond to the BL and clouds. The white regions above 1.5 km in Figs. 5c and 5d were cloud patches. Note that Figs. 5a and 5b are RTIs of the same file only, the color enhancement in Fig. 5b was chosen in such a way as to delineate the cloud tops (much lighter portions) from the CBL. Figs. 5c and 5d are also RTIs of the same file. Note that in Fig. 5d the cloud tops of the thermals (much lighter portions) are made more visible than in Fig. 5c. The convective clouds in Fig. 4b were forced clouds, in which the top portion of the cloud patches could still be seen, while the convective clouds in Fig. 4d were active clouds. Their top portions were no longer detectable and could be much higher than EZ. The dark region above the convective clouds and BL was the FA that was devoid of scatterers.

The normalized covariance of each 30-minute or so array was calculated and superimposed on the RTI map in order to have an immediate comparison between

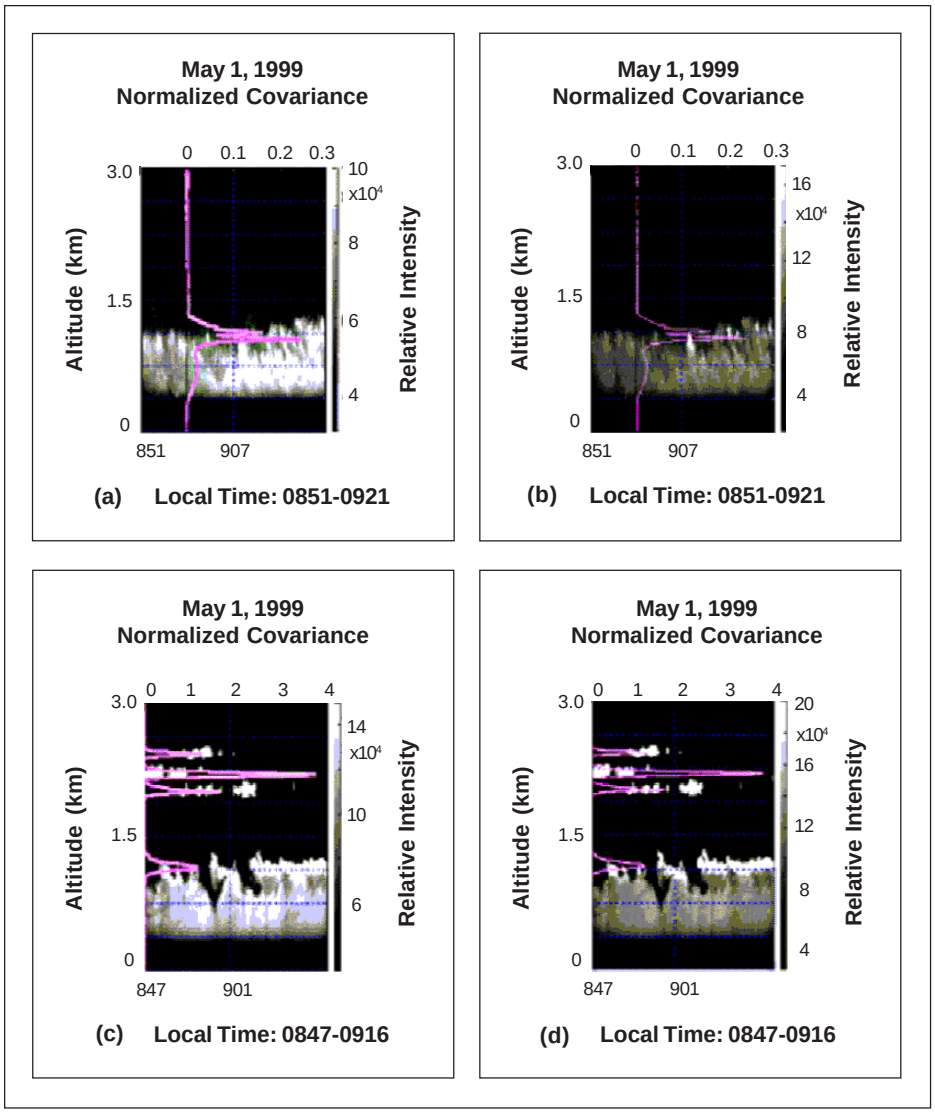

Fig. 5. (a) Processed data for 08:51-09:51 LST on May 1, 1999; (b) The same period as (a) but delineated clouds (red areas) by adjusting the color enhancement scale; (c) Similar to (a) for 08:47-09:16 LST on May 3, 1999; (d) Similar to (b) for the same period as (c).

the manual and the automatic methods of determining the mean CBL height.

The mean CBL height or the base of the inversion layer was estimated using 3 methods, depending on the amount and type of convective cloud cover. If there were no clouds along the lidar beam's path, either above or at the CBL top, the automatic and manual methods described by Hooper & Eloranta (1986), and Piironen & Eloranta (1995) were adopted. In the automatic method, the lowest-altitude local maximum peak of the covariance profile for all data points taken over the 2000 or so lidar profiles was the mean CBL height (Fig. 6c). With the manual or visual method, the height where there was 50% CBL air above and 50% FA air below was taken as the mean CBL top. The horizontal line in Fig. 6c shows this level. This 50-50 level was the definition of Deardorff (1983) of the mean CBL top adopted by Boers & Eloranta (1986), Ferrare et al. (1991), Piironen & Eloranta (1995). Note that the 50-50 level and the peak of the covariance profile are at the same altitude.

If clouds were present along the beam's path as in Fig. 6a, the covariance profile had its maximum at the cloud level, usually making the covariance below it very small. In this case, only the data points below the cloud signals were considered in the recalculation of the covariance. If there is a significant peak in the recalculated covariance profile, that level was taken as the height of the mean CBL as shown in Figs. 6a and 6b. The lowest maximum peak of the covariance profile was taken to be the mean CBL top (horizontal line in Fig. 6b). The bottom-up approach (or choosing the lowest significant peak of the covariance profile) was used to eliminate errors due to strong aerosol variability caused by aerosol layers above the CBL (Piironen & Eloranta, 1995) as in Fig. 6b. The second covariance peak in Fig. 6b pointed by the vertical arrow was due to the variability in the aerosols above the CBL and was not caused by the advection of the dome-shaped tops of the thermals. It is clear from the figure

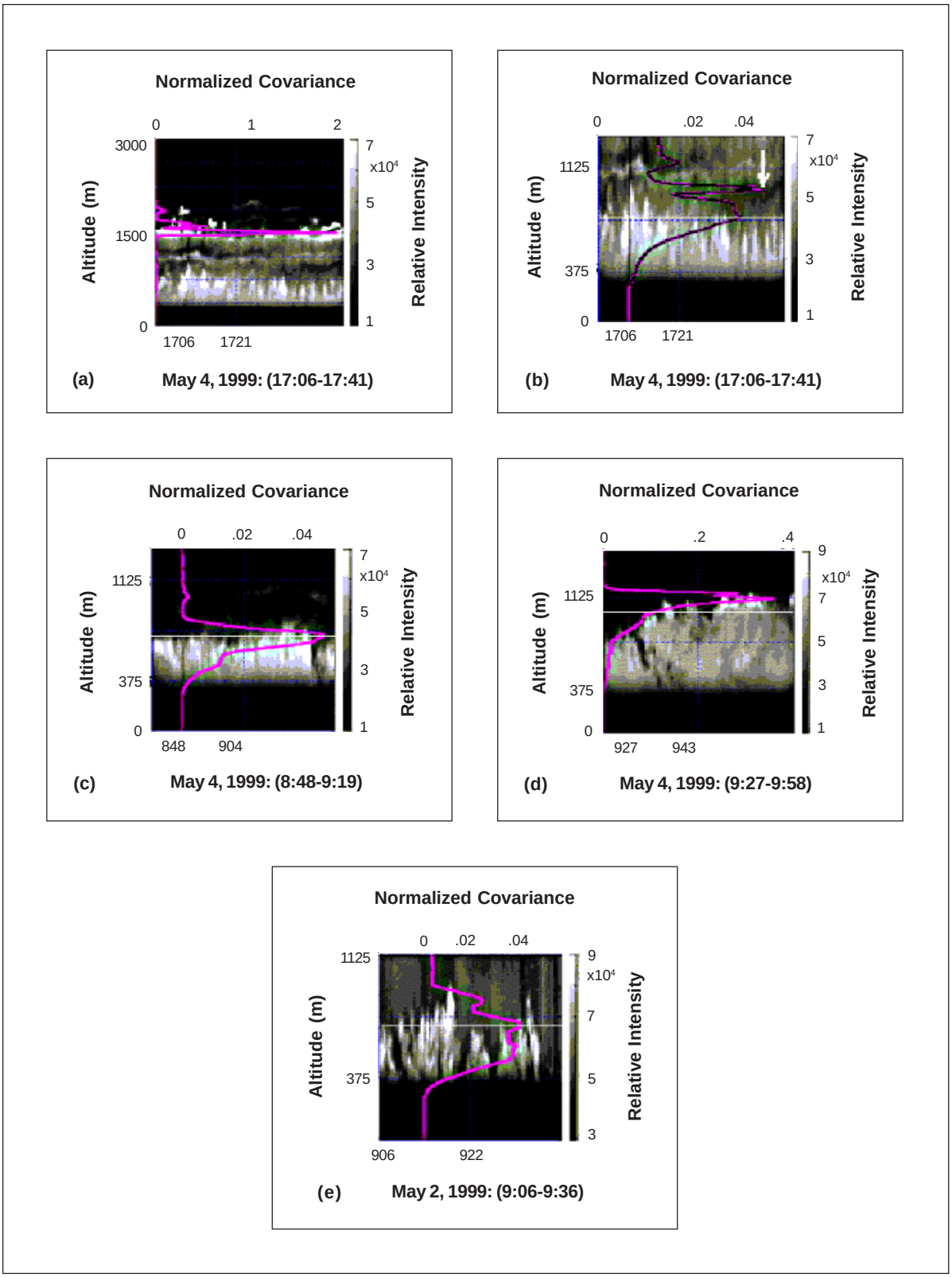

Fig. 6. (a) In the presence of clouds, normalized covariance (Ncov) profile at CBL becomes insignificant; (b) Cloud signals eliminated and Ncov recalculated to reveal Ncov profile at CBL; (c) Ncov profile peaks at CBL mean top if there is no cloud signal; (d) Ncov profile peaks at cloud signal, CBL mean top is at 50-50 level below the Ncov peak; (e) CBL mean top evaluated manually and automatically.

that the thermal tops are way below the second covariance peak. In cases where the covariance profile had multiple peaks (Fig. 6e), the CBL mean top was evaluated manually by visual inspection of the 50-50 level (horizontal line in Fig. 6e) and the result compared with the covariance profile. The covariance peak nearest the 50-50 level was considered as the mean CBL top.

The automatic method could not be used when at least one thermal was cloud-topped since the covariance profile had its maximum at the cloud level, which was more often different from the 50-50 level as shown in Fig. 6d. If the convective cloud cover was forced cloud and cover was less than 10%, the manual method was used. The 50-50 level in Fig. 6d is shown by the horizontal line.

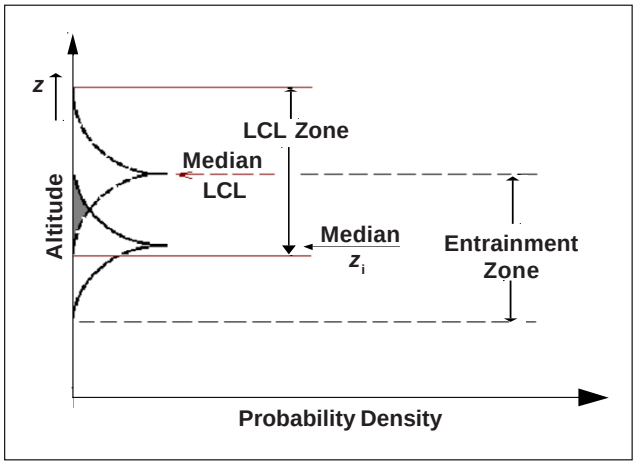

Fig. 7. Relative frequency of occurence of various LCL and mean CBL height z_i in a convective cloud field (Stull, 1988).

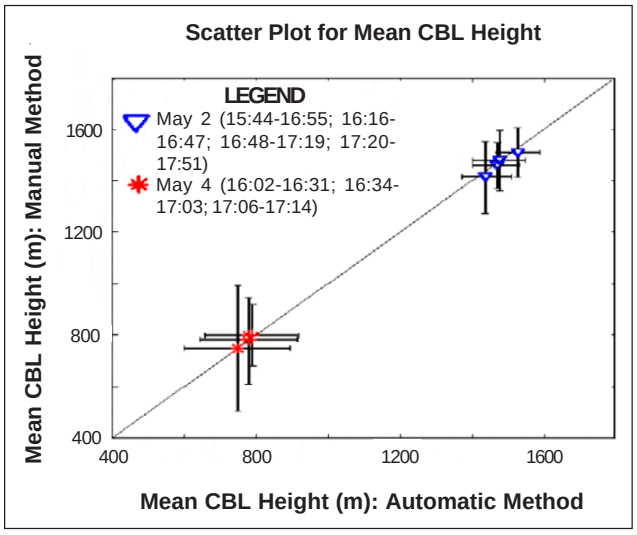

Fig. 8. Scatter plot for the manual and automatic methods of determining the mean CBL height.

If the convective cloud cover was more than 10%, the relationship of the inversion base (or the mean CBL top) and the lifting condensation level (LCL) zone near the base of the convective cloud as defined by Stull (1988) was used. Here, the mean CBL height is around 6% higher than the base of the LCL zone as shown in Fig. 7 (Stull, 1988). The LCL zone was determined from the base of the clouds in the convective cloud field. Because of the subjectivity in evaluating the mean CBL height using the manual and the LCL zone-based methods, RTI images were reevaluated for the mean CBL height at least four times, with succeeding evaluations separated by around one month. Results from one-time evaluation were not very different (up to around 30 m difference) from the previous estimate of the mean CBL height. In cases where both the manual and the automatic methods could be employed to evaluate the mean CBL height, the two methods were both used and the results compared. It was found that the mean CBL height resulting from the two methods agreed very well (Fig. 8).

RESULTS AND DISCUSSIONS

The mean CBL height for the four observation days, 1-4 May 1999 is presented in Fig. 9. There were no measurements at least one hour around noontime. With the sun directly overhead, the photomultiplier tube (PMT) was saturated and no useful data could be taken. The solid lines in Figs. 9a-d denote the mean CBL height for the day. The dashed line in Fig. 9a represents the average height of the part of the CBL without cloud top. This shows that the presence of clouds affects the development of the CBL, which in this case made the mean CBL height lower. The height of the convective cloud, on the other hand is affected by relative humidity. The higher the relative humidity, the lower is the base of the convective cloud, and hence, the lower the mean CBL height. The dashed lines in Figs. 9c and d represent the height of the mixed layer due to sea breeze (Fig. 9)

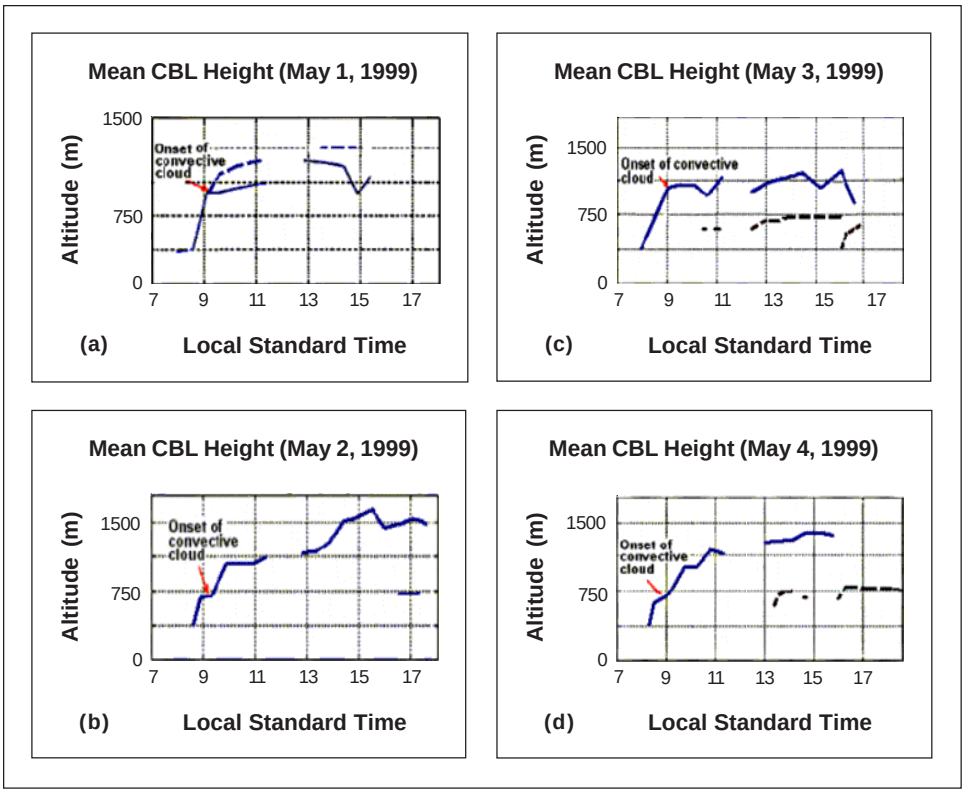

Fig. 9. Time history of the mean CBL height per day for 1-4 May 1999.

and the solid lines, the mean height of the modified CBL.

It can be observed from the different graphs shown in Fig. 9 that the CBL growth, though different each day, has similarities. In general, the CBL growth can be divided into four stages:
(a) Slow CBL growth, which was evident from sunrise until around 08:00 LST;
(b) Rapid CBL growth recorded from around 08:00 LST to mid-morning;
(c) CBL of nearly constant height which occurred between mid-morning and mid-afternoon;
(d) Decay of turbulence, which happened around mid-afternoon until sundown. Here, either the mean CBL height remained the same or decreased a little. In events of prolonged sea breeze a lower mixed layer developed which remained low until sundown.

There may be spatial variations of the CBL heights, but differences may not be very significant if the land cover is more or less uniform over the area as in Metro Manila. Also, it should be remembered that the air sampled over the lidar site was advected from several kilometers from the lidar site – an equivalent of 3840 m for a wind speed of 2 ms^{-1} and 7680 m for a wind speed of 4 ms^{-1} within a 32-min period, the period over which the mean CBL height was estimated. Hence, the derived CBL height over the lidar site can be taken more or less to be the average CBL height over most part of Metro Manila particularly the Loyola Heights and Diliman areas.

The determination of the mean CBL height is a crucial element in understanding the intensity and transport of pollution in the Metropolis. Around 75% of the air pollution in Metro Manila come from traffic emissions (Valeroso et al., 1992; Teodoro, 1998). Traffic volume over most part of Metro Manila especially in main thoroughfares near the lidar site, are seen to peak at around 09:00 LST and a smaller peak between 17:00-18:00 LST, corresponding to the morning and afternoon peak hours. The traffic volume reduces by 20% at around noontime.

The morning peak of the pollution concentration (Fig. 10) occured earlier than that of the traffic. This could be due to the fact that the CBL before 09:00 LST was much lower than after it. Pollution was concentrated in a much lower CBL. The reduction of the pollution concentration on May 1 & 2 was more than twice its morning peak, much higher than expected based on the traffic volume. This could be ascribed to the much higher CBL around noontime. The May 2 pollution profile did not have a peak corresponding to the

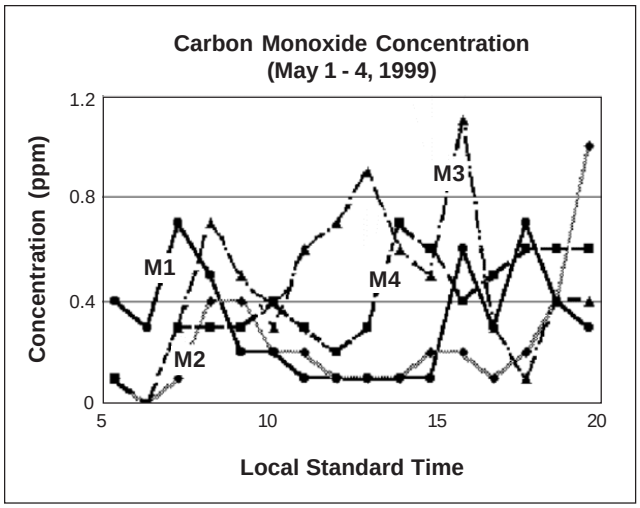

Fig. 10. Diurnal variation of CO concentration on 1-4 May 1999 measured at the lidar site by the UP-NCTS air quality monitoring van.

afternoon peak hour because at that time the mean CBL height was still very high. The May 3 and 4 pollution profiles were different from the two previous days, with values much greater around noontime. Pollution during those times was concentrated in a much lower mixed layer generated by the sea breeze. Figure 11 compares the effect of the much lower mixed layer due to sea breeze on pollution concentration. On May 1 (Fig. 11a), the pollution concentration dropped very significantly at around noontime as a result of the reduction of pollution emission (decreased traffic volume) and the high CBL around that time. On May 3 (Fig. 11b), although there was a reduction in pollution emission, the pollution concentration was much higher at around noontime. This was because of the very low mixed layer due to sea breeze. The very high peak of pollution concentration at 1600 LST on May 3 corresponds to a very low mixed layer that developed at that time. The pollution concentration peak on May 3 occurred earlier than on May 4 (Fig. 10) since the sea breeze was felt at the lidar site much earlier on that day than on May 4. The disproportionate high pollution concentration in the events of sea breeze could also be due partly to the advection of a much polluted air to the lidar site by the sea breeze.

ACKNOWLEDGMENTS

This research study was made possible through the assistance of the Department of Science and Technology (DOST); Ateneo de Manila University (ADMU)–Manila Observatory (MO); Office of the Vice Chancellor for Research and Development (OVCRD), University of the Philippines, Diliman; Philippine Atmospheric, Geophysical, and Astronomical Services Administration (PAGASA); National Center for Transportation Studies (NCTS); Department of Environment and Natural Resources–Environmental Management Bureau; University of the Philippines National Institute of Science and Mathematics Education Development (UP NISMED); the valuable training on lidar data processing and analysis given by

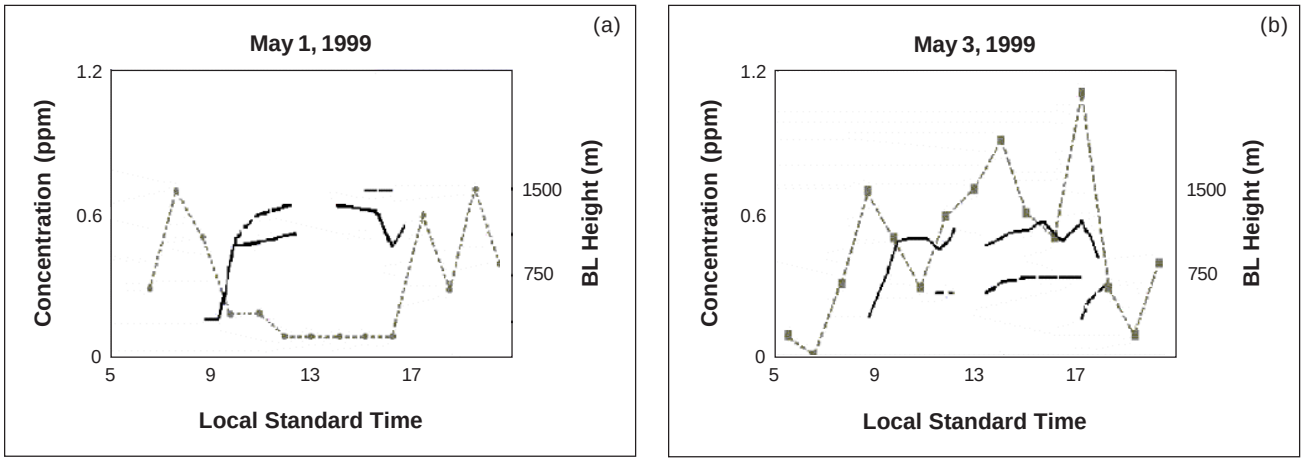

Fig. 11. Pollution concentration profile superimposed on the mean BL height for May 1 and 3, 1999.

Dr. Edwin Eloranta of the University of Wisconsin - Madison to the primary author; initiation of Dr. Minella Alarcon of the existing MO lidar; and the ADMU Lidar Team, especially Anne, Aaron, and C. Enaje for their help in the lidar operations.

REFERENCES

Benkley, C.W., & L.L. Schulman, 1979. Estimating hourly mixing depths from historical meteorological data. *J. Appl. Meteor.* 18:772-780.

Beyrich, F., & S. Gryning, 1998. Estimation of the entrainment zone depth in a shallow convective boundary layer from sodar data. *J. Appl. Meteor*. 37:255-268.

Boers, R., & E.W. Eloranta, 1986. Lidar measurements of the atmospheric entrainment zone and the potential temperature jump across the top of the mixed. *Bound.-Layer Meteor*. 34: 357-375.

Ferrare, R.A., J.L. Schols, E.W. Eloranta, & R.L. Coulter, 1991. Lidar observations of banded convection during BLX83. *J. Appl. Meteor*. 30:312-326.

Hooper, W.P., & E.W. Eloranta, 1986. Lidar measurements of wind in the planetary boundary layer: the method, accuracy and results from joint measurements with radiosonde and kytoon. *J. Climate Appl. Meteor*. 25:990-1000.

Panofsky, H.A., 1985. The planetary boundary layer. *Adv. Geophys*. 28B:359-385.

Piironen, A.K., & E.W. Eloranta, 1995. Convective boundary layer mean depths and cloud geometrical properties obtained from volume imaging lidar data. *J. Geophys. Res*. 100:25 569-25 576.

Stull, R.B., 1988. An introduction to boundary layer metereology. Kluwer Academic Publishers: 647pp.